

# Electrical Drive of a Josephson Junction Array using a Cryogenic BiCMOS Pulse Pattern Generator: Towards a Fully Integrated Josephson Arbitrary Waveform Synthesizer

Yerzhan Kudabay , Oliver Kieler , Michael Starkloff , Marco Schubert , Michael Haas , Johannes Kohlmann , Mark Bieler , and Vadim Issakov 

**Abstract**—We combine a cryogenic BiCMOS integrated circuit, which generates high-speed return-to-zero (RTZ) pulses, with a superconducting Josephson junction array. The BiCMOS circuit acts as a cryogenic pulse pattern generator, delivering data rates of 30 Gb/s, while consuming 302 mW at 4 K. Each electrical pulse of the serializer effectively transfers one magnetic flux quantum through every Josephson junction, so that the average output voltage of the array produces well-defined plateaus (Shapiro steps) in its current-to-voltage characteristic. To the best of our knowledge, this is the first integration of a Josephson junction array with a cryogenic BiCMOS chip. The presented results pave the way toward a hybrid and fully integrated Josephson arbitrary waveform synthesizer (JAWS) that can generate ultra-low-noise signals for quantum voltage metrology and quantum information systems.

**Index Terms**—JAWS, cryogenic IC, Multiplexer, Serializer.

## I. INTRODUCTION

THE development of cryogenic electronics is progressing rapidly [1], driven by the growing demands of quantum technologies and low-temperature applications. A key requirement in this context is the cryogenic implementation of scalable control electronics, with the aim to reduce cabling efforts and the resulting heat insertion into the cryogenic environment. Future quantum computers are expected to incorporate orders of magnitude more qubits than current systems [2]–[4], making scalability a critical design priority. Precise control signals are essential for reliable qubit operation. One possible solution is the use of the JAWS, which is capable of delivering arbitrary frequency- and time-domain signals with extremely high spectral purity.

Previously, JAWS circuits have been shown to synthesize waveforms with extremely high spectral purity, achieving harmonic suppression typically better than -120 dBc [5]–[7]. For quantum voltage metrology applications, these systems deliver an excellent signal-to-noise ratio (SNR), typically ranging from 120 dBc to 140 dBc [7], with a noise floor reaching as low as -140 dBc [6]. These features, combined with low phase noise and high temporal stability, enable the generation

Y. Kudabay and V. Issakov are with the Institute for CMOS Design, Braunschweig University of Technology, Braunschweig, Germany.

O. Kieler, M. Haas, J. Kohlmann and M. Bieler are with the Physikalisch-Technische Bundesanstalt (PTB), Bundesallee 100, 38116 Braunschweig, Germany.

M. Starkloff and M. Schubert are with Supracon AG, Jena, Germany.

Corresponding authors: y.kudabay@tu-braunschweig.de, mark.bieler@ptb.de, v.issakov@tu-braunschweig.de.

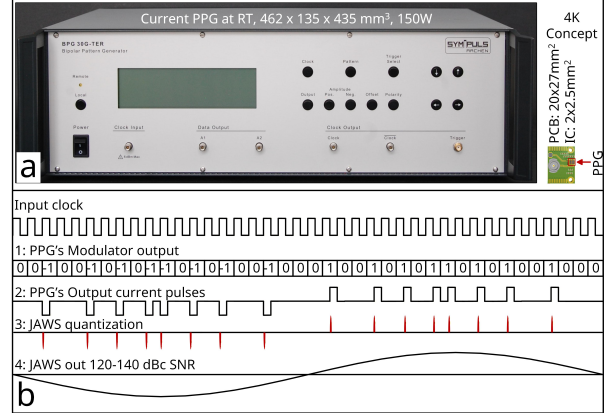


Fig. 1. System realizations: (a) current PPG and 4K concept comparison, (b) Time diagram of the of JAWS operation: (1) serialized and modulated bit-sequence in PPG; (2) output of PPG or input for JAWS; (3) JAWS quantization; (4) JAWS output.

of quantum-accurate arbitrary waveforms from DC up to the MHz range [5], [7].

Typically, the JAWS is realized by driving cryogenic Josephson junction arrays (JJAs) using expensive and bulky 19-inch rack pulse pattern generators (PPGs) held at room-temperature (RT), see Fig. 1a. While in our previous work we have reported only building blocks of integrated PPGs [8]–[10], no experimental results combining a cryogenic integrated circuit (IC) PPG and a JJA for the realization of a JAWS have been published to date.

In this work, we demonstrate the feasibility of combining a JJA with a purpose-designed cryogenic integrated PPG at 4 K to realize a fully integrated JAWS. This is achieved through the use of a compact printed circuit board (20 × 27 mm<sup>2</sup>), incorporating a cryogenic 16:1 serializer together with an array of non-hysteretic Nb/NbSi<sub>x</sub>/Nb Josephson junctions. In the target system architecture, the cryogenic stage will host dedicated ICs for high-speed data generation and serialization, co-integrated with the JAWS, which reduces system complexity, enhances scalability, and minimizes total power consumption—key requirements for operation at 4 K, where cooling capacity is limited. Here, we experimentally demonstrate the BiCMOS 16:1 serializer operating at 30 Gb/s and driving a JJA at 4 K, leading to wide and flat Shapiro steps in the JJA's current-to-voltage characteristics.

It should be noted that the 16:1 serializer employed in

the present work is based on the architecture previously reported in [10]. In contrast to [10], where the serializer was characterized as a standalone cryogenic building block, this work expands the state of the art by demonstrating its integration with a JJA and validating its operation as part of a complete cryogenic pulse pattern generator for JAWS applications Fig. 8.

## II. SYSTEM CONSIDERATIONS

In the following, we briefly summarize the JAWS operation principle from a signal-processing perspective. Conceptually, JAWS behaves like a pulse-density-to-voltage modulator with a quantization (smallest possible voltage step) being defined by superconducting physics. A sequence of current pulses with a time-dependent repetition frequency  $f_p(t)$  is applied to an array of  $N$  Josephson junctions. Each pulse transfers  $M$  flux quanta  $\Phi_0$  through each junction (typically  $M = 1$ ). After low-pass filtering, this produces a quasi-continuous, but quantized, output voltage waveform, as illustrated in Fig. 1b. According to the Josephson relation, the output voltage is given by:

$$V(t) = NM\Phi_0 f_p(t) \quad (1)$$

Here,  $\Phi_0 = h/2e$  is the magnetic flux quantum,  $h$  is Planck's constant, and  $e$  is the elementary charge. It is important to note that  $\Phi_0$  is a fixed constant, so the average output voltage is directly set by the number of junctions  $N$ , the number of quanta  $M$  per pulse, and the pulse repetition frequency  $f_p(t)$ . This enables JAWS to synthesize voltage waveforms with very fine, inherently quantized resolution. In contrast to conventional AC quantum voltage standards that generate sinusoidal waveforms with a rich harmonic spectrum, JAWS performs quantization directly in the time domain, which strongly suppresses harmonic distortion and allows clean and precise waveform generation.

The root-mean-square (RMS) value of the generated voltage can be calculated using:

$$V_{\text{signal(RMS)}} = A_{\Sigma\Delta} NM\Phi_0 f_{\text{clock}} \quad (2)$$

where  $A_{\Sigma\Delta}$  is the amplitude coefficient of the sigma-delta ( $\Sigma\Delta$ ) modulation, with  $0 < A_{\Sigma\Delta} < 1$ . The signal frequency is determined by:

$$f_{\text{signal}} = T_{\Sigma\Delta} \frac{f_{\text{clock}}}{L_{\Sigma\Delta}} \quad (3)$$

with  $T_{\Sigma\Delta}$  being the number of signal periods in the code,  $L_{\Sigma\Delta}$  being the length of the sigma-delta sequence, and  $f_{\text{clock}}$  being the fixed clock frequency of the PPG.

Typically, JAWS utilizes superconductor - normal conductor - superconductor (SNS) Josephson junctions due to their non-hysteretic current voltage (I-V) characteristics under microwave excitation, i.e., they do not exhibit memory effects between switching events. In pulse-mode operation, properly chosen pulse amplitudes and repetition rates create pronounced Shapiro steps, which appear as flat voltage plateaus in the I-V curve of the junction array [7]. Large and stable Shapiro steps are obtained when the pulse repetition frequency  $f_p$  is on the order of the junction's characteristic frequency  $f_c$ .

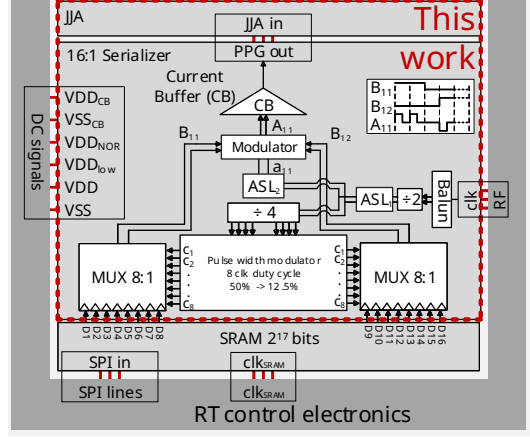


Fig. 2. Block diagram of the PPG.

In practice,  $f_p$  for JAWS operation typically lies in the 15–20 GHz range, limited by the capabilities of commercial PPGs, see Fig. 1a [11]. This corresponds to data rates of approximately 30–40 Gb/s, assuming that two data bits (1 and 0) form one return-to-zero pulse.

## III. THE CIRCUIT DESIGN

The concept for our hybrid integration of the JJA and the BiCMOS chip comprises two stages. The first stage, located at RT, contains low-frequency control electronics. The second stage, located at 4 K, integrates the cryogenic PPG IC with the JJA. In the target system architecture, summarized in Fig. 2, the PPG will employ a dedicated external memory chip and a clock-generation block, which locally provide a long  $\Sigma\Delta$ -modulated bit sequence to the serializer. The memory chip contains  $2^{17}$  bits to enable fine frequency resolution and to avoid continuous data and heat transfer from RT. This memory IC, implemented using SRAM, has already been developed and tested with the serializer, but was not integrated with the serializer in the current prototype. In this work, only the high-speed 16:1 serializer, modulator, and clock-distribution network are integrated on the BiCMOS chip, while the bit-pattern generation is realized externally at RT.

In our target system the JAWS requires a stream of high-speed input pulses to operate correctly; therefore, the cryogenic PPG must support comparable data rates. The overall system architecture is depicted in Fig. 2. A 16:1 serializer operating at 30 Gb/s is used between the SRAM and JAWS.

The generation of clear eye diagrams requires precise clock and data signals alignment, as misalignment can induce sampling at incorrect points of the bit period, thereby compromising signal integrity, as it is depicted in Fig. 3.

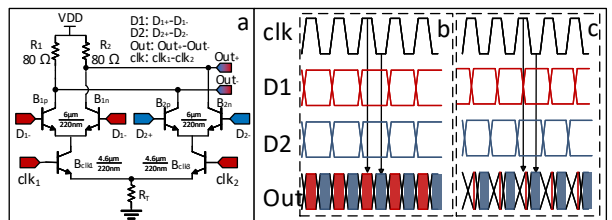


Fig. 3. Synchronization issue: (a) 2:1 CML MUX, (b) aligned data and clocks signals, (c) misaligned data and clocks signals.

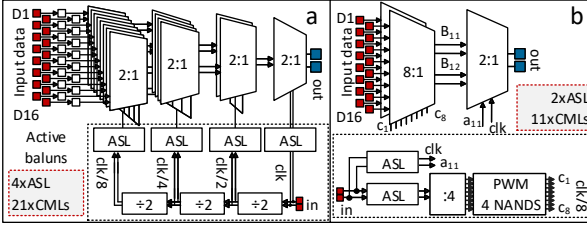


Fig. 4. 16:1 MUX realizations (a) 2:1 MUX based 16:1 MUX, (b) 8:1 MUX based 16:1 MUX.

In conventional high-speed systems, timing synchronization is typically achieved through calibrated delay calculations, which are performed under well-defined operating conditions (temperature and frequency). In contrast, the system developed in this work is designed to operate across a wide temperature range, from 4 K to RT, and data rates, from 10 to 30 Gb/s, depending on the system requirements. This design flexibility enables preliminary validation at RT before the 4 K measurements, thereby streamlining the characterization process.

The lack of accurate cryogenic component models makes it impossible to apply conventional delay modeling techniques, which depend on temperature-sensitive models. To overcome this limitation and ensure robust timing alignment across operating conditions, the design incorporates Active Synchronization Lines (ASLs), which provide a tunable and scalable solution for maintaining phase alignment between critical timing signals.

#### A. 8:1 MUX

The 16:1 serializer consists of two 8:1 MUXes using the same clock signals and provide non-return-to-zero output signals to modulator. The comparison of the conventional 16:1 MUX (a) with based on two 8:1 MUXes (b) is depicted on Fig. 4. The diagram shows that the conventional approach requires 21 current-mode logic (CML) devices and 4 ASLs with four distinct frequencies, while the new realization needs 2 ASLs with two frequencies and 11 CML devices, highlighting the new design power efficiency and simplicity.

The 8:1 MUX schematic, depicted in Fig. 5a, comprises four cells, each implemented as two differential pairs stacked with two clock-controlled transistors. The differential pair function as active balun, where one transistor is driven by the input data via CMOS inverters, which were utilized for logic level compatibility (SRAM output swing 0-0.8 V and CMOS

inverter 0-1.5 V), while the complementary transistor is biased at a fixed voltage  $V_{b2} = 1.3$  V.

The clocking transistors in the 8:1 MUX are controlled by a 12.5% duty cycle clock signals, from  $C_1$  to  $C_8$  as depicted on Fig. 5, enabling sequential latch operation. A single tail current source is shared across all clocking transistors, ensuring that only one differential pair is active at any given time. This 8:1 MUX design simplifies the overall MUX topology and reduces power consumption.

#### B. Clock distribution network

The clock distribution network generates eight phase-shifted (45°) clock signals with a 12.5% duty cycle at one-eighth the input clock frequency for the 8:1 MUXes. It also provides a clock signal for the NOR gate in the modulator at half the input frequency. The network has ASLs, static frequency dividers, and a pulse width modulator (PWM) to convert duty cycle from 50% to 12.5%.

The delay cell is a differential pair with tunable load impedance, enabling delays up to 50% of the signal period in the 5-24 GHz range. To meet this requirement without excessively increasing the load impedance, each ASL cascades nine delay cells. The load is controlled via an external voltage for tuning flexibility—higher voltages result in longer delays. A PMOS current source (P1) and NMOS current mirror (N1-N4) ensure stable output amplitude.

The CML frequency dividers reduce the input clock frequency by 8, producing eight synchronized 50% duty cycle clock signals with 45° phase separation. The PWM transforms the 50% duty cycle outputs from the divider into 12.5% duty cycle clock signals, as shown on Fig. 5b. Conventionally, eight NAND gates are used, with one output per gate being utilized since one output has 12.5% duty cycle and second 87.5%. The proposed NAND cell generates two outputs, differential signals with 12.5% duty cycle, allowing to use only four cells.

#### C. Modulator

The modulator comprises two NAND gates and modified NOR gate, which generates a RTZ bipolar signal. The employed modulation has a 50% shorter pulse duration than conventional PAM modulations. The +1 and -1 symbols are represented by the “10” and “01” bit patterns, respectively. The NOR gate is driven by a clock signal from the ASL, operating at the same frequency as the primary input clock.

## IV. MEASUREMENTS

The 16:1 serializer chip, occupying an area of  $2 \times 2.5 \text{ mm}^2$  and fabricated in Infineon’s 0.13  $\mu\text{m}$  SiGe B11HFC BiCMOS process, is shown in Fig. 6c. The chip was characterized under multiple operating conditions, including RT, a cryogenic probe station, and at 4 K using both a cryocooler (Fig. 6a,b) and liquid helium (LHe) immersion. Cryogenic measurements required extended cabling and additional adapters between the RT and cryogenic stages, resulting in increased insertion losses and reduced signal integrity, which limited precise tuning of supply and tuning voltages for optimum serializer operation.

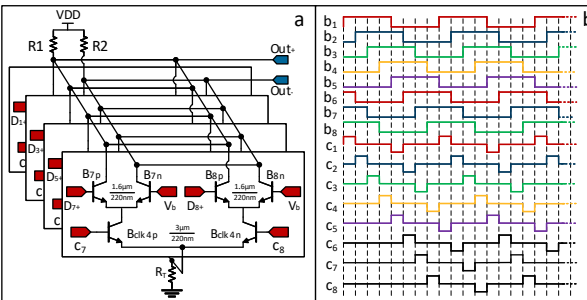


Fig. 5. (a) 8:1 MUX schematic, (b) 12.5% clock generation.

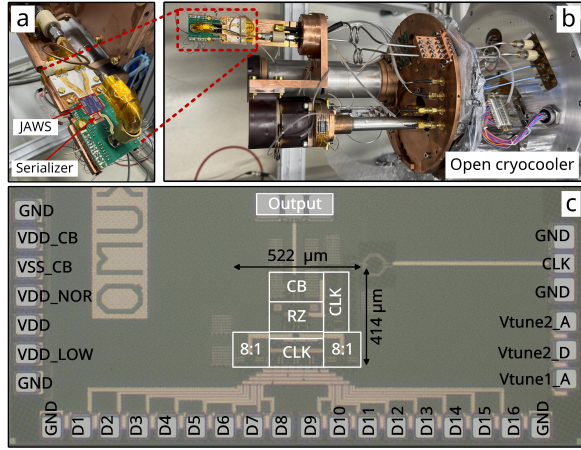


Fig. 6. (a) Carrier with mounted JJA and serializer, (b) opened cryocooler with mounted chips, (c) PPG microphoto.

The output eye diagrams measured at RT and 4 K, shown in Fig. 7a and Fig. 7b, exhibit a noticeable degradation at cryogenic temperatures. This behavior is attributed to temperature-dependent changes in the dielectric properties of substrate and interconnect materials, leading to overshoot, ringing, and steeper signal transitions that increase inter-symbol interference. Fig. 7 summarizes the measured 30 Gb/s output eye diagrams with a 50% duty cycle, corresponding to a power consumption of 306 mW at RT and 436 mW at 4 K.

During the joint measurements of the serializer and the JJA, a resistive heater was employed to accurately determine the serializer power consumption under operating conditions in which the serializer successfully drove the JJA. The heater consisted of precision resistors with a resistance of  $121.7\Omega$ , through which a controlled DC current was driven. The resulting heating was used to dissipate a well-defined amount of power directly into the copper mounting plate with the chips, thereby providing a calibrated thermal load. The results presented in Fig. 8 were obtained at a serializer power consumption of 302 mW in cryocooler and 360 mW in liquid helium (LHe), while the maximum serializer power consumption,

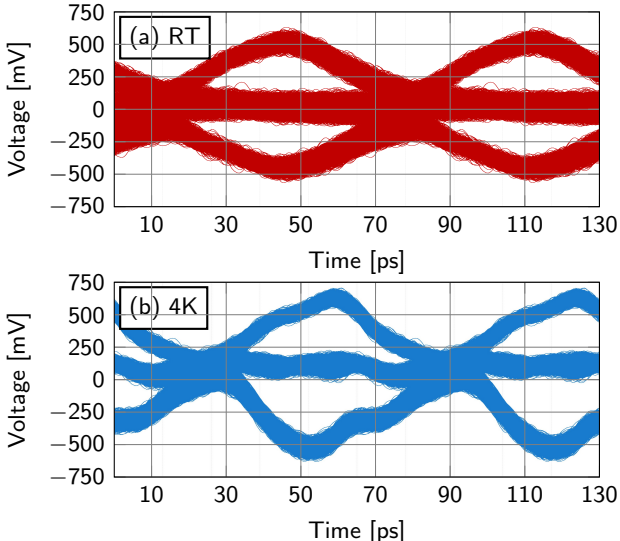


Fig. 7. Serializer measurement results at 30 Gb/s (a) RT, (b) 4 K.

at which serializer operation was verified, was approximately 600 mW, where it provided wider Shapiro Steps.

The JJAs used in this work comprise an array of 150 and 7494 Josephson junctions, embedded in the center line of a coplanar waveguide, which was matched to  $50\Omega$  impedance. The JJA chips have dimensions of  $10 \times 10 \text{ mm}^2$  and was fabricated in PTB's clean-room (ISO class 5). More details about fabrication of JAWS and JJA used in this work can be found in [7], [12]. The devices exhibits a critical current of  $I_c = 4.3 \text{ mA}$  for the smaller array and  $I_c = 5.8 \text{ mA}$  for the bigger array, a normal-state resistance of  $R_n = 3.1 \text{ m}\Omega$ , a characteristic voltage of  $V_c = 13.5 \text{ }\mu\text{V}$ , and a corresponding characteristic frequency of  $f_c = 6.5 \text{ GHz}$ . In our experiments, the chosen operating points ensure that the serializer pulses remain within a regime where the JJA exhibits wide and flat Shapiro steps at the targeted data rates.

The performance of the JJAs and the BiCMOS serializer was evaluated under cryogenic conditions using both a LHe dewar and a cryocooler, thereby demonstrating the robustness and reproducibility of the joint JJA and serializer measurements.

For the cryocooler-based measurements, the serializer and the JJA comprising 7494 Josephson junctions were mounted on a dedicated copper carrier, shown in Fig. 6a, which was subsequently installed inside the cryocooler, as illustrated in Fig. 6b. The serializer PCB was equipped with an RF connector to provide the high-frequency clock signal. Electrical isolation of the JJA was ensured by integrated on-chip inner and outer DC blocks.

For the LHe measurements, a JJA consisting of 150 Josephson junctions and the BiCMOS serializer were mounted on two separate Rogers PCBs, each equipped with two RF connectors. The boards were attached to a cryogenic probe stick and interconnected by a short 10 cm coaxial cable to transmit the serializer output signal to the JJA. The remaining connectors were used to supply the clock signal to the serializer and to

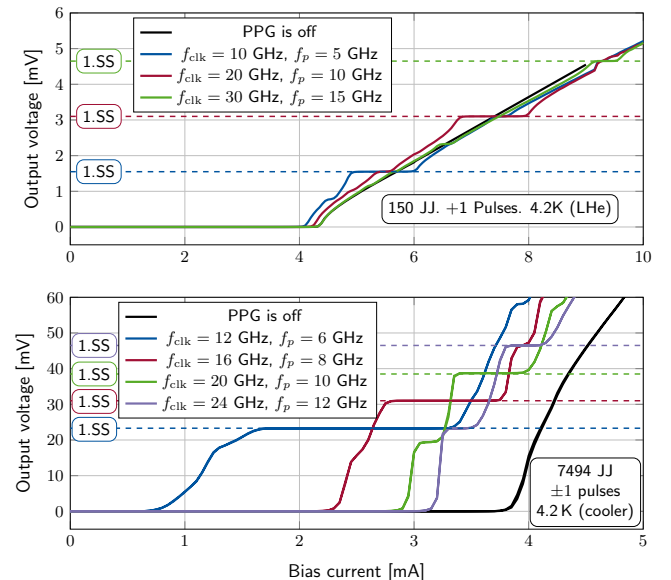


Fig. 8. Current-voltage characteristics of serializer and JJAs joint measurements (a) in a cryo-cooler and (b) in liquid Helium.

TABLE I  
MUX STATE-OF-THE-ART COMPARISON

	This	[9]	[14]	[15]	[16]
Data Rate @RT, Gb/s	30	24	40	50	64
Data Rate @Cryo, Gb/s	30	24	36	-	-
Technology process	130nm BiCMOS	130nm BiCMOS	40nm CMOS	16nm CMOS	28nm CMOS
Function	16:1	8:1	64:1	16:1	4:1
Stages	2	1	3	4	3
Power @RT, mW	306	224	88.8	243	135
Power @Cryo, mW	302	-	98.6	-	-
Area, mm <sup>2</sup>	0.217	0.132	0.146	0.2	0.12

provide mechanical fixation. Electrical isolation was achieved using inner and outer DC blocks.

The supply voltages, input data, and control signals were soldered directly to the PCBs in both measurement setups and interfaced with external power supplies at RT. Fixed bit patterns were applied as input data during all measurements.

The results of the joint cryogenic measurements are summarized in Fig. 8. Pronounced Shapiro steps are observed for the JJA with 150 junctions in LHe at data rates of 10 Gb/s, 20 Gb/s, and 30 Gb/s, as well as for the JJA with 7494 junctions in cryocooler at 12 Gb/s, 16 Gb/s, 20 Gb/s, and 24 Gb/s. The presence of wide and well-defined Shapiro steps confirms that the serializer output signal is sufficiently preserved when transferred to the JJA chips under cryogenic conditions with different measurement setups, different JJAAs and at different frequencies. Remarkably, we also observe fractional Shapiro steps at  $M = 1/2$ , most likely due to an interaction of the microwave signal, being incident on the Josephson junctions, with the phase oscillations occurring in the junctions [13].

To the best of our knowledge, no system combining a high-speed cryogenic driver with JAWS or JJA has been reported in the literature thus far with this level of integration. Nevertheless, Table I summarizes the measurement obtained at RT and cryogenic temperatures for serializer's, providing a comparison with the state-of-the-art of serializers. Only few operate at cryogenic temperatures.

## V. CONCLUSION

This work presents a proof-of-concept and the first successful JJA integration with high-speed cryogenic BiCMOS 16:1 serializer IC. The system exhibits a wide and flat Shapiro steps, demonstrates the feasibility of co-integrating classical high-speed control electronics with superconducting quantum standards. The serializer's wide temperature (from 4 K up to RT) and data rate (up to 30 Gb/s) ranges highlight the importance of robust clock distribution at cryogenic temperatures for future quantum metrology and information systems.

## ACKNOWLEDGMENTS

The authors thank the German Federal Ministry of Research, Technology, and Space (BMFTR) for financial support in QuMIC project (grant agreements 13N15932 and 13N15934).

## REFERENCES

- [1] P. Toth, P. Shine Eugine, Y. Kudabay, K. Yamashita, S. Halama, J. Parvizinejad, M. Bonkowski, H. Ishikuro, C. Ospelkaus, and V. Issakov, "A Cryo-BiCMOS Controller for Quantum Computers based on Trapped Beryllium Ions," *IEEE Journal of Solid-State Circuits*, pp. 1–17, 2025.
- [2] S. Chakraborty and R. V. Joshi, "Cryogenic CMOS Design for Qubit Control: Present Status, Challenges, and Future Directions [Feature]," *IEEE Circuits and Systems Magazine*, vol. 24, no. 2, pp. 34–46, 2024.
- [3] J. Anders, M. Babaie *et al.*, "CMOS Integrated Circuits for the quantum information sciences," *IEEE Transactions on Quantum Engineering*, vol. 4, pp. 1–30, 2023.
- [4] J. P. G. v. D. Xue, B. Patra *et al.*, "CMOS-based cryogenic control of silicon quantum circuits," *Nature*, vol. 593, p. 205–210, May 2021.
- [5] N. E. Flowers-Jacobs, A. Rüfenacht, A. E. Fox, S. B. Waltman, R. E. Schwall, J. A. Brevik, P. D. Dresselhaus, and S. P. Benz, "Development and Applications of a Four-Volt Josephson Arbitrary Waveform Synthesizer," in *2019 IEEE International Superconductive Electronics Conference (ISEC)*, 2019, pp. 1–2.
- [6] R. Behr, O. Kieler, J. Lee, S. Bauer, L. Palafox, and J. Kohlmann, "Direct comparison of a 1 V Josephson arbitrary waveform synthesizer and an ac quantum voltmeter," *Metrologia*, vol. 52, no. 4, p. 528, jun 2015. [Online]. Available: <https://doi.org/10.1088/0026-1394/52/4/528>
- [7] O. Kieler, "Development of josephson arbitrary waveform synthesizer at Physikalisch-Technische Bundesanstalt (PTB)," *Low Temperature Physics*, vol. 50, no. 11, pp. 948–961, 11 2024. [Online]. Available: <https://doi.org/10.1063/10.0030410>
- [8] Y. Kudabay and V. Issakov, "A 0.03 mm<sup>2</sup> inductorless 50 gb/s multiplexer for josephson arbitrary waveform synthesizers," in *2022 IEEE BiCMOS and Compound Semiconductor Integrated Circuits and Technology Symposium (BCICTS)*, 2022, pp. 124–127.
- [9] Y. Kudabay, P. J. Ritter, and V. Issakov, "A Single-Stage 24 Gb/s 8:1 Cryogenic Multiplexer for Josephson Arbitrary Waveform Synthesizer," in *2024 IEEE BiCMOS and Compound Semiconductor Integrated Circuits and Technology Symposium (BCICTS)*, 2024, pp. 58–61.
- [10] Y. Kudabay, P. J. Ritter, and V. Issakov, "A Cryogenic 30 Gb/s PAM3 BiCMOS Serializer for Josephson Arbitrary Waveform Synthesizer," in *2025 20th European Microwave Integrated Circuits Conference (EuMIC)*, 2025, pp. 113–116.
- [11] "BPG30G-TER Product Page," Online, 2025, sympuls Aachen, available: <https://www.sympuls-aachen.de/produkte/bpg30g-ter/bpg30g-ter-en.html>.
- [12] O. F. Kieler, R. Behr, R. Wendisch, S. Bauer, L. Palafox, and J. Kohlmann, "Towards a 1 V Josephson Arbitrary Waveform Synthesizer," *IEEE Transactions on Applied Superconductivity*, vol. 25, no. 3, pp. 1–5, 2015.
- [13] O. V. Karpov, V. M. Buchstaber, S. I. Tertychniy, J. Niemeyer, and O. Kieler, "Modeling of rf-biased overdamped Josephson junctions," *Journal of Applied Physics*, vol. 104, no. 9, p. 093910, 11 2008. [Online]. Available: <https://doi.org/10.1063/1.3008011>
- [14] N. Fakkil, M. Mortazavi, R. Overwater, F. Sebastian, and M. Babaie, "A Cryo-CMOS DAC-based 40 Gb/s PAM4 Wireline Transmitter for Quantum Computing Applications," in *2023 IEEE Radio Frequency Integrated Circuits Symposium (RFIC)*, 2023, pp. 257–260.
- [15] H. Chandrakumar, T. W. Brown, D. Frolov, Z. Tuli, I. Huang, and S. Rami, "A 48dB-SFDR, 43dB-SNDR, 50GS/s 9-bit 2x-interleaved Nyquist DAC in Intel 16," in *2022 IEEE Custom Integrated Circuits Conference (CICC)*, 2022, pp. 1–2.
- [16] E. Depaoli, H. Zhang, M. Mazzini, W. Audoglio, A. A. Rossi, G. Albasini, M. Pozzoni, S. Erba, E. Temporiti, and A. Mazzanti, "A 64 Gb/s Low-Power Transceiver for Short-Reach PAM-4 Electrical Links in 28-nm FDSOI CMOS," *IEEE Journal of Solid-State Circuits*, vol. 54, no. 1, pp. 6–17, 2019.